JPET Fast Forward. Published on April 15, 2005 as DOI: 10.1124/jpet.105.084517

JPET #84517

Title: In situ naphthalene bioactivation and nasal airflow cause region-specific injury patterns in the nasal mucosa of rats exposed to naphthalene by inhalation

Authors: Myong Gyong Lee, Andrew Phimister, Dexter Morin, Alan Buckpitt, and Charles Plopper

Primary laboratories of origin: Department of Anatomy, Physiology, and Cell Biology, School of Veterinary Medicine, University of California, Davis, California (M.G.L., A.P., C.P.); and Department of Molecular Biosciences, School of Veterinary Medicine, University of California, Davis, California (D.M., A.B.)

JPET #84517

Running title: Acute injury from inhaled naphthalene in rat nose

Address correspondence to:

Myong Gyong Lee

One Shields Avenue

Department of Anatomy, Physiology, and Cell Biology

School of Veterinary Medicine

University of California

Davis, CA 95616

Telephone: (530) 752-1174; Fax: (530) 752-7690

Email: mglee@ucdavis.edu

Number of text pages: 31

Number of tables: 0

Number of figures: 6

Number of references: 28

Number of words

Abstract: 245; **Introduction:** 591; **Discussion:** 1360

List of nonstandard abbreviations: NA, naphthalene; CYP450, cytochrome P450; DMM, dorsal medial meatus; MMM, middle medial meatus; LOAEL, lowest observable adverse effect level; OSHA, Occupational Safety & Health Administration

Recommended section assignment: Toxicology

Abstract

Despite the fact that naphthalene (NA), a volatile, ubiquitous air pollutant, was recently identified as a probable human carcinogen, little is known about nasal cytotoxicity from inhaled NA. To define and compare acute nasal injury from inhalation and systemic NA exposures, male Sprague Dawley rats were exposed to filtered air, 3.4 ppm, or 23.8 ppm NA by inhalation for 4 hours or to 0, 25, 50, 100, or 200 mg/kg NA via intraperitoneal injection. Severe cellular injury occurred exclusively in the olfactory mucosa 24 hours post inhalation exposure to 3.4 ppm NA for 4 hours. This level is significantly below both the current OSHA standard (10 ppm, 8 hours) for NA and the LOAEL (10 ppm, 2 years) for the incidence of rat olfactory neoplasms. Injury within the olfactory mucosa from inhaled NA was confined to the medial meatus, whereas systemic NA generated severe injury throughout the olfactory region. The pattern of nasal injury from inhaled NA in this study is consistent with previous studies of nasal airflow simulation within the olfactory region. The non-olfactory mucosa on the nasal septum, a high airflow region, metabolized naphthalene slowly, whereas the olfactory regions of the nasal septum and ethmoturbinates metabolized this substrate at high rates. This study concludes that: 1) the incidence of acute nasal injury from systemic and inhaled NA correlates with the rates of regional microsomal NA metabolism and that 2) the nasal airflow pattern determines the pattern of olfactory mucosal injury from inhaled NA.

Introduction

As a first entry point of inhaled compounds, the nasal passage is at risk of being injured by a number of air pollutants like NA. The mammalian nasal passage is lined with four different epithelial populations: squamous, transitional (non-ciliated cuboidal/columnar), respiratory, and olfactory epithelium. Among these, the olfactory mucosa (i.e., the olfactory epithelium and its underlying lamina propria) contains four primary cells: the duct cells lining Bowman's glands, basal cells, olfactory receptor cells, and the sustentacular cells or olfactory supporting cells. Of these, the acinar cells lining Bowman's glands and the sustentacular cells are particularly rich in xenobiotic-metabolizing enzymes such as CYP450s (See review: Thornton-Manning and Dahl, 1997). Therefore, the olfactory mucosa has the potential to metabolize protoxicants that require *in situ* bioactivation. Toxic metabolites generated in the nasal passage could pass into the systemic circulation due to the rich vasculature and high perfusion rate of the nasal region (Ding and Dahl, 2003). Likewise, the nasal passage could be an injury target for xenobiotics undergoing systemic circulation (Placke et al., 1987; Gu et al., 1997).

Previous studies have shown that the olfactory mucosa of the rat is a major target of NA toxicity by intraperitoneal administration (≥ 200 mg/kg NA, both the LOAEL and the lowest dose of their trial), and NA injury occurred uniformly across the olfactory region (Plopper et al., 1992). Bioactivation of NA by CYP450s to NA-1,2-epoxide is a key event in a series of steps leading to cytotoxicity (Buckpitt et al., 1995). For a number of species, including non-human primates, nasal tissue, especially olfactory mucosa, contains high concentrations of CYP450s. In humans, significant expression/activity of CYP450s in the

nasal mucosa have been reported. For example, in the olfactory mucosa of humans, CYP2A6 and CYP2A13 are highly expressed and are catalytically active towards a number of toxicants including tobacco-specific nitrosamines (Chen et al., 2003; Su et al., 2000).

NA is volatile (0.082 mmHg at 25ºC) and insoluble in water (31.7 mg NA in 1 L water at 20ºC) (Verschueren, 1983). A major route of NA exposure in humans is via inhalation. A concentration dependent increased incidence of nasal neoplasms was noted following inhalation exposure of rats to NA for 2 years even at the lowest concentration tested (10 ppm; National Toxicology Program, 2000). Recently, the International Agency for Research on Cancer (2002) categorized NA as a category 2B carcinogen (possibly carcinogenic to humans).

This study was designed to examine mucosal injury to the rat nasal passage from acute exposure to NA by inhalation. Our preliminary inhalation data indicated that olfactory mucosal injury was not uniform within the mucosa after inhalation exposure to NA, and this contrasts with the more uniform distribution of injury observed following systemic administration of NA. The hypothesis tested in this study was that the non-uniform pattern of olfactory mucosal injury from acute NA exposure by inhalation is due to both nasal airflow patterns and regional differences in NA bioactivation. In order to test the hypothesis, the goals were 1) to define the nasal pattern of injury from inhaled NA at doses which are substantially lower and higher than the current OSHA standard for NA, 2) to compare the nasal injury pattern from inhaled NA with the results of previous studies on nasal airflow patterns by examining transverse sections of the rat nasal passage, 3) to compare the nasal injury pattern from inhaled NA with that from NA administered

intraperitoneally, and 4) to determine whether the patterns of nasal injury from inhaled NA reflect the potential for regional bioactivation of NA microsomes from nasal tissue.

Methods

Chemicals. The following chemicals were used: naphthalene (> 99 % purity; Fisher Scientific, Gibbstown, NJ); glycol methacrylate resin (Electron Microscopy Sciences, Fort Washington, PA); acetonitrile (EMD Chemicals, Gibbstown, NJ); triethylamine (Burdick & Jackson Division, Muskegon, MI); β-nicotinamide adenine dinucleotide phosphate hydrate (β-NADP); L-glutathione, glucose-6-phosphate, glucose-6-phosphate dehydrogenase (Sigma-Aldrich, St. Louis, MO); paraformaldehyde (Fisher Scientific, Gibbstown, NJ); formic acid (Merck KgaA, Darmstadt, Germany); and Toluidine blue (Polysciences, Warrington, PA).

Animals. Male Sprague Dawley rats were purchased from Harlan Laboratories (San Diego, CA). Animals were provided with food and water *ad libitum* and were housed in an AAALAC accredited facility in HEPA-filtered cages at the University of California, Davis, for at least 7 days before use in an experiment. Rats weighed 180-200 g at the time of necropsy.

Inhalation Exposures. Three treatment groups of 6 rats each were exposed to filtered air, 3.4 ± 0.5 ppm NA, and 23.8 ± 1.7 ppm NA. All rats were exposed for 4 hours. Exposures were done from 10 am to 2 pm to minimize the effect of diurnal fluctuation of glutathione (Jaeschke and Wendel, 1985) on the extent of NA injury. Glass metabolism cages (Bioserve, Laurel, MD) housed 2 rats during the inhalation period. Rats were allowed free access to water while in the chamber. The desired NA concentrations inside the chamber were achieved by adjusting the flow rates of fresh air and the air flowing through a glass column (2.5 x 60 cm) packed with NA crystals. The air supply (medical air; Puritan Medical Products, Overland Park, KS) passed through an activated carbon

filter prior to use in the chamber. Both fresh air and NA-containing air were mixed in a separate glass flask before entering the chamber. Total airflow inside the chamber was maintained at 1 L min^{-1} throughout the exposure period, which resulted in a complete air exchange every 5 min. The temperature of the chamber was maintained at 25 ºC. Ten ml of air inside the chamber was removed using a gas-tight syringe (Hamilton, Reno, NV) and then dissolved in 3 ml of acetonitrile. Extraction efficiency of NA into acetonitrile was 80.0%. The concentrations of NA dissolved in acetonitrile were monitored by UV absorbance at 219.2 nm using an extinction coefficient of 89,100 M^{-1} cm^{-1}. A conversion factor (1 ppm = 5.24 mg/m^3 at 25°C) (International Agency for Research on Cancer, 2002) was applied in order to obtain a concentration of NA in the gas phase as parts per million (ppm).

Intraperitoneal administration of NA. Rats received a dose of 0, 25, 50, 100, or 200 mg of NA/kg of body weight in corn oil (Mazola, Cordova, TN) by intraperitoneal injection. Each group consisted of 3 rats. All rats were treated between 11 am to noon to minimize the influence of diurnal fluctuation of glutathione on the extent of NA injury.

Necropsy and Sample Preparation for High-resolution Histopathology. Rats were euthanized with an overdose of sodium pentobarbital 24 hours following inhalation or intraperitoneal NA exposures. The animals were exsanguinated by cutting the abdominal aorta. After the lower jaw was removed, the head was separated from the cadaver. The nasal passage was fixed in 40 ml of 4 % paraformaldehyde (0.1 M sodium phosphate buffer, pH 7.4) at 4 ºC for at least 24 hours after being flushed with 5-6 ml of ice-cold 4% paraformaldehyde through the nasopharyngeal duct. The fixed nasal passage was decalcified in 40 ml of 13% formic acid with gentle shaking for 5 days at room

temperature. The decalcified nasal passage was washed with running tap water for 4 hours and was grossly sectioned perpendicular to both the nose bridge and the nasal septum at the following four specific anatomic locations (Young, 1981; Mery et al., 1994): (1) immediately posterior to the upper incisive teeth, (2) through the incisive papilla, (3) through the second palatal ridge, and (4) in the middle of the first upper molar teeth. The sections were embedded in glycol methacrylate. Two to three micron sections were generated from each embedded section using a Zeiss Microme HM340E microtome (Carl Zeiss, Thornwood, NY). Sections were stained with 1% Toluidine blue for examination by high-resolution light microscopy. For the purposes of this study, level 7 (L7) and level 23 (L23) were chosen. The levels were based on a diagram of the cross-sections of the entire nasal passage of the rat by Mery et al. (1994) that has 30 cross-sections. L7 and L23 mimic the cross-sections where the airflow studies (Kimbell et al., 1997) have provided detailed information of nasal airflow, and the NTP bioassay reported incidence of neoplasm (adenoma and neuroblastoma).

High-resolution Light Microscopic Quantification of Injury. To quantify NA injury within the olfactory region along the basement membrane, the length of the basement membrane lined with injured and uninjured olfactory epithelium was measured with *Scion Image* (Scion, Frederick, MD). Results are expressed as a percent of basement membrane lined with injured olfactory epithelium.

Microsomal Incubations. To determine whether the characteristic injury pattern from inhaled NA in the rat nasal passage reflected the differences in regional formation of NA-1,2-epoxide from NA, microsomes were prepared from nasal tissue isolates. Sampling sites were chosen based on nasal airflow patterns and the injury patterns from inhaled NA

(See results for more details of sampling sites.) Each sample was pooled from 14 unexposed rats. Samples were washed with ice-cold buffer (200 mM Tris/1.15% KCl, pH 7.4 at 4°C) after removal. All samples were homogenized similarly using a Polytron homogenizer (Glen Mills, Clifton, NJ). Microsomes were prepared by differential centrifugation at 9,000*g* for 30 min at 4°C followed by centrifugation of the supernatant at 100,000*g* for 65 min at 4°C. Measurement of active microsomal CYP450s was performed as described by Schenkman and Jansson (1999). Microsomal protein concentration was determined according to Bradford (1976), with bovine serum albumin as the standard.

NA-1,2-epoxide was trapped as glutathione conjugates by using optimized concentrations of glutathione and glutathione S-transferases (Buckpitt et al., 1992). Incubations were prepared on ice in a final volume of 200 µl. Each incubation consisted of 100 mM sodium phosphate buffer (pH 7.4), 15.4 pmoles of active CYP450s, 0 to 160 µM of NA, 1 mM reduced glutathione, 6 CDNB units glutathione S-transferases, and a NADPH-generating system. The NADPH-generating system was added to give a final concentration of 0.22 mM NADP, 6.2 mM glucose-6-phosphate, 0.1 unit glucose 6-phosphate dehydrogenase, and 15 mM $MgCl_2$. The NADPH-generating system was pre-incubated for 2 min at 37°C to ensure the presence of NADPH at the onset of incubation, and then it was added into the incubations on ice. NA solutions were prepared in methanol and added to the incubation mixture at 0.5% (v/v). Incubations were allowed to proceed for 10 min at 37°C in 12 x 35 mm capped glass vials (with Teflon PTFE-lined closures; Fisher Scientific, Gibbstown, NJ) in a shaking water bath. The reactions were

terminated by adding 400 µl ice-cold methanol, and samples were stored at - 20°C overnight or longer. All incubations were prepared in triplicate or quadruplicate.

HPLC Analysis of NA Metabolites. This analysis was done as in Buckpitt et al. (1987) except that the acetonitrile gradient was modified. Terminated incubation mixtures were centrifuged at 13,000g for 30 min at -4ºC to pellet the precipitated protein. The supernatant was collected and evaporated under a vacuum to complete dryness. Dried samples were stored at -80°C until HPLC analysis. Samples were reconstituted in 100 µl water and centrifuged to remove particulates. NA glutathione conjugates and diol were separated on a Phase Sep C_{18} ODS2 column (250 x 4.6 mm i.d.; 5-µm particle) (Waters, Milford, MA). The eluates were monitored by UV absorbance at 260 nm. A mobile phase of 0.06% triethylamine phosphate in water (pH 3.1) and acetonitrile was used at a flow rate of 1.0 ml/min with a linear increase from 10 to 14% acetonitrile over 60 min. Metabolites of NA were identified by comparing retention times with synthesized NA metabolite standards. NA metabolites were quantified against a standard curve of synthetic NA metabolite standards. Synthesized NA metabolites were made by conjugating NA oxide with glutathione and were purified by HPLC. They were stored at -80 ºC until use.

Statistics. All data were imported into *Prism 3.0* (GraphPad, San Diego, CA) for statistical analysis. Differences in percentage of injured area among the groups of filtered air, 3.4 ppm NA, and 23.8 ppm NA were determined by one-way analysis of variance (ANOVA) using the Bonferroni's post-hoc test. Differences in V_{max} for the formation of NA metabolites from the microsomal incubation of the septal olfactory mucosa versus ethmoturbinates were determined by unpaired t-test.

Results

I. Nasal injury from inhaled naphthalene (NA) correlates with the airflow patterns in the nasal passage of rats

In the anterior region of the nasal passage (L7), olfactory mucosa is present in the dorsal medial meatus (DMM). In the posterior region of the nasal passage (L23), olfactory mucosa lines the area of the DMM, along the nasal septum, and most of the ethmoturbinates (Figure 1a, olfactory mucosa marked in green) (Mery et al., 1994). The olfactory epithelium of rats exposed to filtered air was not injured (Figures 2a and 3a). The top of the olfactory epithelium was covered with fine cilia extending from the olfactory receptor cells, and most of the nuclei in the epithelial layer were from pseudostratified olfactory receptor cells. Cytoplasm from sustentacular cells was situated between the cilia and nuclei of the olfactory epithelium. After NA inhalation, injury was found only in the olfactory mucosa. At 3.4 ppm NA, the continuity of the olfactory mucosa in L7 and L23 was broken by areas of necrotic olfactory receptor cells, the volume of cytoplasm from sustentacular cells above the nuclei was reduced, and vacuoles were present in the olfactory epithelial layer (Figures 2b and 3b). At this dose, L7 also had patches of exfoliated cells. This other type of cellular damage indicated that the injury was more severe at L7 compared to at L23 (Figure 2c versus 3b). The frequency for the incidence of both types of injury at L7 from 3.4 ppm NA appeared to be the same. After exposure to 23.8 ppm NA, numerous exfoliated cells and cell debris were trapped in the nasal passage at both levels (Figures 2d and 3c). However, the specific area of the DMM at L23 showed less injury (Figure 3d) compared to the rest (Figure 3c) of the olfactory region of L23. Despite the presence of numerous intraepithelial vacuoles and

the reduced volume of cytoplasm from sustentacular cells of the DMM at L23 after 23.8 ppm NA exposure, the height of the epithelium was still preserved, and the nuclei from epithelial cells were visible within the epithelial layer of the DMM at L23. Basal cells of the olfactory mucosa appeared to remain unaffected in all of the NA treated rats. In the underlying lamina propria of injured olfactory mucosa at both levels, the Toluidine blue staining for seromucous materials in the Bowman's glands appeared to be depleted by NA treatment. However, both nerve bundles and blood vessels looked the same in NA treated rats as in filtered air treated rats.

Regional patterns of olfactory mucosal injury were focal (Figure 1a, injury marked in blue). At 3.4 ppm NA, injury was confined around the DMM of the nasal passage at both L7 and L23. At 23.8 ppm NA, injury at L23 further extended ventrally along the medial meatus. That is, not only was the olfactory mucosa lining the DMM injured but also those cells lining the nasal septum and medial aspects of the ethmoturbinates. In some rats, one half of the nasal passage, which is divided by the nasal septum, showed a preferential distribution of injury. This was the case at L23 for three out of six rats exposed to either concentration of NA. There was a significant increase ($*p < 0.001$) in the length of the basement membrane lined with injured olfactory epithelium after NA exposure, and this effect was concentration dependent in both L7 and L23 (Figure 1b).

In general, it appeared that the pattern of injury from inhaled NA correlated well with the computational fluid dynamics-based model of nasal airflow patterns by Kimbell et al. (1997). At L23, olfactory mucosal injury from inhaled NA primarily occurred within the medial meatus of the nasal passage where the majority of the nasal airflow is allocated (approximately 81-92% of total airflow passing through L23 above the

nasopharyngeal duct) after exposure to 23.8 ppm NA. At L23, olfactory mucosal injury from the lower dose (3.4 ppm) of NA was confined to the very first pathway of inspiratory nasal airflow at L23, the dorsal half of the medial meatus. Injury from either dose of NA by inhalation exposure was not observed in the low airflow area, mostly along the ethmoturbinates. Kimbell et al. (1997) reported that not only the airflow allocation but also the speed decreases along the stream of nasal air as inhaled air moves through the nasal passage. The degree of injury from inhaled NA was more severe at L7 than at L23 when we examine the DMM, where nasal air flows from L7 towards L23 direction.

II. Comparison of nasal injury following inhalation and systemic exposure to NA

Cross sections of L7 and 23 from the nasal passage of rats treated intraperitoneally with varying doses of NA were prepared and examined in the same manner as the NA inhalation study. No mucosal injury was observed in the rats injected with 0, 25, or 50 mg/kg of NA, and their mucosa looked similar to that in rats exposed to filtered air by inhalation at L7 and L23 (Figures 2a and 3a). However, at 100 and 200 mg/kg NA, cellular injury was apparent. Systemic exposure to NA generated widespread injury in the olfactory mucosa at L7 (not shown) and L23 (Figure 4g). In contrast to the pattern of injury observed after NA inhalation, injury occurred not only along the medial meatus but also throughout the ethmoturbinates at L23. The degree of olfactory mucosal injury decreased in a posterior to anterior direction through the nasal passage (not shown).

Similar to what was seen with inhalation exposure, at L23, injury in the DMM was milder compared to the rest of the olfactory region of rats treated with 100 mg/kg NA; the only signs of injury were occasional degeneration of sustentacular cell cytoplasm and the presence of intraepithelial vacuoles (Figure 4a). In contrast, the rest of the olfactory epithelium in L23 had extensive exfoliation (Figure 4b). At 200 mg/kg NA, however, severe cellular exfoliation was uniform throughout L23 (Figures 4c and 4d). Basal cells were included in the population of exfoliated epithelium from systemic NA (Figures 4b and 4d), which was not apparent after inhalation exposure. Unlike inhaled NA, there was not a tendency for preferential distribution of injury in one half of nasal passage over the other. Another prominent difference between inhalation and systemic exposure was the presence of large vacuoles and loss of cilia in ciliated columnar cells, non-olfactory epithelium, along the lateral walls of L23 at ≥ 100 mg/kg NA (Figure 4e versus 4f). Similar to NA inhalation exposure, seromucous materials in the Bowman's glands were depleted by systemic NA treatment, and both nerve bundles and blood vessels appeared unaffected by NA.

III. NA metabolism from regional nasal microsomal incubations

Three sampling sites for microsomal incubation of NA were chosen based on nasal airflow patterns and the injury patterns from inhaled NA: 1) the olfactory mucosa of the nasal septum (high airflow area), 2) the ethmoturbinates from both sides of the nasal passage (mostly lined with olfactory mucosa; mostly low airflow area), and 3) the non-olfactory region of the nasal septum (mostly lined with non-olfactory mucosa; high airflow area). The most dorsal ethmoturbinate was not used in order to avoid the chance

of including any mucosa from the dorsal medial meatus. The levels of CYP450 by nasal region were 267 ± 11, 278 ± 17, and 74 ± 9 pmoles/mg of microsomal protein for the septal olfactory region, the ethmoturbinates, and the septal non-olfactory region, respectively. Figure 5 summarizes the regional differences in rates of metabolism of NA (160 μM) in microsomes isolated from rat nasal mucosa. The majority of NA metabolites generated in microsomal incubations were glutathione conjugates of NA-1,2-epoxide in all three nasal regions. A small portion of NA-1,2-epoxide was metabolized to 1,2-dihydroxy-1,2-dihydronaphthalene by microsomal epoxide hydrolase (4.1%, 6.9%, and 2.8%) for the septal olfactory region, the ethmoturbinates, and the septal non-olfactory region, respectively) instead of being conjugated with glutathione. Four diastereomeric glutathione conjugates were generated, and 1R-hydroxy-2R-glutathionyl-1,2-dihydronaphthalene, derived from 1R,2S-naphthalene oxide, was the primary metabolite for all three nasal regions. The percent of total metabolites accounted for by 1R-hydroxy-2R-glutathionyl-1,2-dihydronaphthalene was 77.7% for the septal olfactory region and 72.6% for the ethmoturbinates and the septal non-olfactory region. The average rate of microsomal metabolism (the combined rate for the formation of both glutathione conjugates and dihydrodiol) of NA (0 to 160 μM) by nasal region is shown in Figure 6.

Discussion

The results of this study indicate that cellular injury in the olfactory mucosa of the rat occurs after only 4 hours of exposure to 3.4 ppm naphthalene (NA), a dose considerably lower than the current OSHA standard for NA [10 ppm for 8 hour time-weighted average with a standard threshold exposure concentration of 15 ppm]. Severe nasal injury occurred exclusively in the olfactory region after exposure to inhaled and systemic NA. The data from this study demonstrate that the only areas of the nasal mucosa severely injured after either systemic or inhalation exposures of NA are those capable of metabolizing NA. However, within the olfactory area at L23, inhaled NA generated olfactory mucosal injury patterns which were region-specific compared to those observed after systemic administration of NA. These data suggest that acute injury from inhaled NA results from *in situ* metabolism of NA rather than NA metabolites delivered from extranasal tissues. Within the olfactory regions, the nasal airflow pattern determines the pattern of olfactory mucosal injury from inhaled NA. High rates of NA bioactivation by nasal microsomes raises the possibility that the nasal tissue of humans may be an injury target of NA since significant expression/activity of CYP450s in the nasal mucosa have been reported in humans (Longo et al., 1989; Gervasi et al., 1991; Gu et al., 2000; Su et al., 2000; Chen et al., 2003).

The National Toxicology Program's bioassay (2 year inhalation of NA) has reported an exposure-related incidence of neuroblastoma in the olfactory region and adenoma in the respiratory and transitional epithelia of the anterior part of the nasal cavity along the medial or lateral aspects or tips of the nasoturbinates in the nasal passage of Fisher F344/N rats. In the current study, we were unable to observe cellular injury in

the non-olfactory mucosa of the nasoturbinates. However, a significant degree of olfactory mucosal injury occurred below the LOAEL (10 ppm, female and 30 ppm, male) for nasal carcinoma (neuroblastoma) in the 2 year bioassay conducted by the National Toxicology Program.

One of the goals of this study was to determine whether nasal injury from inhaled NA is related to simulated airflow patterns. The studies of computational fluid dynamics on nasal airflow patterns in rats have shown that 15-19% of the total inspiratory airflow reaches the olfactory region at L7 while at L23 this decreases to 3-8% of the total inspiratory airflow (Kimbell et al., 1997). Of the airflow reaching the olfactory region at L23, approximately 90% moves through the dorsal half of the medial meatus. Once this air reaches the back of the nasal passage, it changes direction and about 85% flows towards the anterior region through a narrow passage, the ventral half of the medial meatus at L23. Shortly thereafter, the air changes direction again and joins the major inspiratory airflow from the nostril directly towards the nasopharyngeal duct. Therefore, the allocation of nasal airflow in the wide area of the lateral parts at L23, mostly along the ethmoturbinates, is quite small.

Previous studies examining the susceptibility of the nasal mucosa of rats have shown that the formaldehyde mass flux predicted by computer fluid dynamics techniques correlates with both the patterns of non-olfactory mucosal injury from inhaled formaldehyde (Kimbell, 1993) and the sites of DNA-protein cross-linking induced by inhaled formaldehyde (Hubal, 1997). Hardisty et al. (1999) have found that eight toxicants (propylene glycol monomethyl ether acetate, n-butyl propionate, ethyl acetate, n-butyl acetate, dibasic esters, primary amyl acetate, vinyl acetate, or methyl

methacrylate) result in a consistent pattern of olfactory mucosal injury after inhalation exposure, regardless of concentration and duration of exposure. The olfactory mucosal injury was confined to the medial meatus (high airflow area). In addition, Moulin et al. (2002) found that, following 70 days of exposure of rats to hydrogen sulfide (30 or 80 ppm), nasal injury occurred only within the olfactory mucosa. The patterns of olfactory mucosal injury correlated with the high-deposition sites of inhaled hydrogen sulfide predicted by computational fluid dynamics techniques. However, the remaining nasal regions did not show such correlations. Olfactory mucosal injury from inhaled hydrogen sulfide was also confined within the medial meatus, which is similar to what was observed from inhaled NA. However, mechanisms involved in toxification and/or detoxification for most of the aforementioned compounds including hydrogen sulfide are unknown.

Since the balance between generation and detoxification of reactive metabolites is likely to be an important determinant in site selective toxicity, another goal of this study was to examine regional differences in NA bioactivation as a possible reason for the specific injury patterns observed after exposure to naphthalene vapors. Buckpitt et al. (1995) have previously correlated the formation of NA-1,2-epoxide by CYP450s and its consequent cytotoxicity in lung tissues. Current data indicated that the average velocity (V) (the combined rate for the formation of both glutathione conjugates and 1,2-dihydroxy-1,2-dihydronaphthalene from NA-1,2-epoxide per mg of microsomal protein) at the highest substrate concentration tested (160 μM) was not significantly different between the septal olfactory region and the ethmoturbinates ($p < 0.05$). The rates of microsomal naphthalene metabolism were similar at the remaining NA concentrations

(Figures 6a and 6b). Similar rates of bioactivation may explain why the degree of injury was indistinguishable between the septal olfactory mucosa and ethmoturbinates when NA (≥ 100 mg/kg) was administered intraperitoneally since it should distribute uniformly within the olfactory area when delivered via the vasculature. However, the dependence on airflow patterns would explain why injury from inhaled NA primarily occurred in the septal olfactory mucosa. The presence of multiple P450 isoforms which are able to bioactivate NA in the nasal mucosa precluded classic kinetic analyses.

Injury from NA in the DMM at L23 was more severe with inhalation (23.8 ppm NA) than with systemic exposure (100 mg/kg NA) (Figure 3d versus 4a), indicating that more NA reached the olfactory mucosa in the DMM at L23 via the inhalation route (23.8 ppm NA) compared to the systemic route (100 mg/kg NA). Nevertheless, olfactory mucosal injury in the low airflow area (mostly ethmoturbinates) at L23 was observed only from systemic NA (100 mg/kg NA) not from inhaled NA (23.8 ppm NA). This suggests that in the olfactory area at L23, a clear difference in the injury patterns from NA depends on the amount of NA delivered by the exposure route. Therefore, within the olfactory area (septal olfactory region and ethmoturbinates), differences in airflow (as predicted in simulations) appeared to govern the injury patterns from inhaled NA rather than just *in situ* formation of NA-1,2-epoxide.

NA was metabolized at a higher rate by the septal olfactory region and ethmoturbinates than the septal non-olfactory region (Figures 5 and 6). In the septal non-olfactory region (high airflow region), it is likely that most of the NA metabolism came from the small isolated patch of olfactory mucosa situated in the septal non-olfactory mucosa (the organ of Masera (Weiler and Farbman, 2003); covering approximately 3%

of the septal non-olfactory region by surface area). Severe injury of this small olfactory patch from inhaled NA was apparent at either concentration of NA when the nasal septum was examined by scanning electron microscopy (not shown). Therefore, virtually no NA bioactivation occurs in the septal non-olfactory mucosa, which is consistent with the finding that no cellular injury was observed in the septal non-olfactory mucosa regardless of the route of exposure or concentration of NA.

Less severe injury was noted in the dorsal medial meatus (DMM) of the olfactory region at L23, regardless of the route of exposure (Figures 3d and 4a). The small sample size precluded isolation of sufficient tissue for analysis of metabolic rates.

In conclusion, the current study found that 1) nasal injury in rats from inhaled and systemically administered NA was cell-type specific and occurred primarily in the olfactory mucosa, 2) olfactory mucosal injury was region-specific, and the regional patterns of olfactory mucosal injury were significantly different depending on exposure routes i.e., inhalation versus intraperitoneal injection, 3) the incidence of acute nasal injury from systemic and inhaled NA correlates with regional microsomal formation of NA-1,2-epoxide , and 4) regional patterns of olfactory mucosal injury from inhaled NA correlate with the regions of highest airflow based on previous simulation studies in the rat nasal passages.

Acknowledgements

The authors appreciate Dr. Suzette Smiley-Jewell for help editing the manuscript. We are also grateful to Dr. Michael Evans, Dr. Michelle Fanucchi, and Bridget Boland for critical reading, Chad Fleschner for initial help in animal treatment and processing, and Dr. Gregory Baker for help with statistical analysis.

References

Bradford MM (1976) A rapid and sensitive method for the quantitation of microgram quantities of protein utilizing the principle of protein-dye binding. *Anal Biochem* **72**:248-254.

Buckpitt AR, Castagnoli N Jr, Nelson SD, Jones AD and Bahnson LS (1987) Stereoselectivity of naphthalene epoxidation by mouse, rat, and hamster pulmonary, hepatic, and renal microsomal enzymes. *Drug Metab Dispos* **15**:491-498.

Buckpitt A, Chang AM, Weir A, Van Winkle L, Duan X, Philpot R and Plopper C (1995) Relationship of cytochrome P450 activity to Clara cell cytotoxicity. IV. Metabolism of NA and NA oxide in microdissected airways from mice, rats, and hamsters. *Mol Pharmacol* **47**:74-81.

Buckpitt A, Boland B, Isbell M, Morin D, Shultz M, Baldwin R, Chan K, Karlsson A, Lin C, Taff A, West J, Fanucchi M, Van Winkle L and Plopper C (2002) NA-induced respiratory tract toxicity: metabolic mechanisms of toxicity. *Drug Metab Rev* **34**:791-820.

Chen Y, Liu Y, Su T, Ren X, Shi L, Liu D, Gu J, Zhang Q and Ding X (2003) Immunoblot analysis and immunohistochemical characterization of CYP2A expression in human olfactory mucosa. *Biochem Pharmacol* **66**:1245-1251.

Ding X and Dahl A (2003) Olfactory mucosa: composition, enzymatic localization, and metabolism in *Handbook of Olfaction and Gustation*, 2nd ed (Doty RL ed) pp 51-73, Marcel Dekker, New York.

Gervasi PG, Longo V, Naldi F, Panattoni G and Ursino F (1991) Xenobiotic-metabolizing enzymes in human respiratory nasal mucosa. *Biochem Pharmacol* **41**:177-184.

Gu J, Su T, Chen Y, Zhang QY and Ding X (2000) Expression of biotransformation enzymes in human fetal olfactory mucosa: potential roles in developmental toxicity. *Toxicol Appl Pharmacol* **165**:158-162.

Gu J, Walker VE, Lipinskas TW, Walker DM and Ding X (1997) Intraperitoneal administration of coumarin causes tissue-selective depletion of cytochromes P450 and cytotoxicity in the olfactory mucosa. *Toxicol Appl Pharmacol* **146**:134-143.

Hardisty JF, Garman RH, Harkema JR, Lomax LG and Morgan KT (1999) Histopathology of nasal olfactory mucosa from selected inhalation toxicity studies conducted with volatile chemicals. *Toxicol Pathol* **27**:618-627.

Harkema JR, Hotchkiss JA, Barr EB, Bennett CB, Gallup M, Lee JK and Basbaum C (1999) Long-lasting effects of chronic ozone exposure on rat nasal epithelium. *Am J Respir Cell Mol Biol* **20**:517-529.

Hubal EA, Schlosser PM, Conolly RB and Kimbell JS (1997) Comparison of inhaled formaldehyde dosimetry predictions with DNA-protein cross-link measurements in the rat nasal passages. *Toxicol Appl Pharmacol* **143**:47-55.

International Agency for Research on Cancer (IARC) (2002) Monographs on the evaluation of carcinogenic risks to humans: some traditional herbal medicines, some mycotoxins, NA and styrene. Vol 82, IARC, Lyon, France.

Jaeschke H and Wendel A (1985) Diurnal fluctuation and pharmacological alteration of mouse organ glutathione content. *Biochem Pharmacol* **34**:1029-1033.

Kimbell JS, Gross EA, Joyner DR, Godo MN and Morgan KT (1993) Application of computational fluid dynamics to regional dosimetry of inhaled chemicals in the upper respiratory tract of the rat. *Toxicol Appl Pharmacol* **121**:253-263.

Kimbell JS, Godo MN, Gross EA, Joyner DR, Richardson RB and Morgan KT (1997) Computer simulation of inspiratory airflow in all regions of the F344 rat nasal passages. *Toxicol Appl Pharmacol* **145**:388-398.

Longo V, Pacifici GM, Panattoni G, Ursino F and Gervasi PG (1989) Metabolism of diethylnitrosamine by microsomes of human respiratory nasal mucosa and liver. *Biochem Pharmacol* **38**:1867-1869.

Mery S, Gross EA, Joyner DR, Godo N and Morgan KT (1994) Nasal diagram: a tool for recording the distribution of nasal lesions in rats and mice. *Toxicol Pathol* **22**:353-372.

Moulin FJ, Brenneman KA, Kimbell JS and Dorman DC (2002) Predicted regional flux of hydrogen sulfide correlates with distribution of nasal olfactory lesions in rats. *Toxicol Sci* **66**:7-15.

National Toxicology Program (NTP) (2000) Toxicology and Carcinogenesis Studies of NA (CAS No. 91–20-3) in F344/N Rats (Inhalation Studies), in *NTP Technical Report No. 500; NIH publication No. 01–4434*, Research Triangle Park, NC.

Placke ME, Wyand DS and Cohen SD (1987) Extrahepatic lesions induced by acetaminophen in the mouse. *Toxicol Pathol* **15**:381-387.

Plopper CG, Suverkropp C, Morin D, Nishio S and Buckpitt A (1992) Relationship of cytochrome P-450 activity to Clara cell cytotoxicity. I. Histopathologic comparison of the respiratory tract of mice, rats and hamsters after parenteral administration of NA. *J Pharmacol Exp Ther* **261**:353-363.

Schenkman JB and Jansson I (1999) Measurement of cytochrome P-450, in *Current Protocols in Toxicology* (Maines MD ed) pp 4.1.1-4.1.14, John Wiley & Sons, Hoboken, NJ.

Su T, Bao Z, Zhang QY, Smith TJ, Hong JY and Ding X (2000) Human cytochrome P450 CYP2A13: predominant expression in the respiratory tract and its high efficiency metabolic activation of a tobacco-specific carcinogen, 4-(methylnitrosamino)-1-(3-pyridyl)-1-butanone. *Cancer Res* **60**:5074-5079.

Thornton-Manning JR and Dahl AR (1997) Metabolic capacity of nasal tissue interspecies comparisons of xenobiotic-metabolizing enzymes. *Mutation Res* **380**:43-59.

Verschueren K (1983) *Handbook of environmental data on organic chemicals,* 2nd ed pp 118-119, Van Nostrand Reinhold Co., New York.

Weiler E and Farbman AI (2003) The septal organ of the rat during postnatal development. *Chem Senses* **28**:581-593.

Young JT (1981) Histopathologic examination of the rat nasal cavity. *Fundam Appl Toxicol* **1**:309-312.

Footnotes

a) This work was supported by the National Institute of Environmental Health Sciences Grants ES04311, ES04699 and ES06700. University of California Davis is a National Institute of Environmental Health Sciences Center in Environmental Health (ES05707), and support for core facilities used in this work is gratefully acknowledged. A portion of this work was presented in the 43rd Annual Meeting of Society of Toxicology held 21-25 March, 2004 in Baltimore, Maryland, USA

b) The name and full address of the person receiving reprint requests:

Myong Gyong Lee

One Shields Avenue

Department of Anatomy, Physiology, and Cell Biology

School of Veterinary Medicine

University of California

Davis, CA 95616

Legends for figures

1. Regional patterns of mucosal injury from NA inhalation at two representative cross sections of the nasal passage, L7 (a, b, and c) and L23 (d, e, and f). L7 is the anterior region of the nasal passage, while L23 is the posterior region. Rats were exposed to filtered air, 3.4 ppm NA, or 23.8 ppm NA. The location of olfactory mucosa is marked in green, injured areas in blue, and areas of the DMM are shadowed in pink. Significant cellular injury from inhaled NA occurred primarily along the medial meatus of the nasal passage; Magnification bar = 800 μm. There was a significant increase (*$p < 0.001$) in the percent of basement membrane lined with injured olfactory epithelium in accordance with increasing concentration of inhaled NA at the cross sections of both L7 (g) and L23 (h) of the nasal passage.

2. Cellular injury in the olfactory mucosa from inhaled NA at L7 along the DMM.in rats exposed to (a) Filtered air, (b) 3.4 ppm NA, (c) 3.4 ppm NA, and (d) 23.8 ppm NA. Arrowheads indicate the basement membrane. Negative undulation is marked by arrows. Cilia from olfactory receptor cells (**C**); sustentacular cells (**S**); olfactory receptor cells (**O**); basement membrane (**bm**); Bowman's glands (**bg**); arterioles (**a**); venuoles (**v**); nerve bundle (**n**); nasal septum (**ns**); vacuoles (******). Magnification bars = 50 μm.

3. Cellular injury from inhaled NA at L23. (a) Filtered air in the olfactory region at L23, (b) 3.4 ppm NA in the dorsal medial meatus (DMM), (c) 23.8 ppm NA in the ventral two-third's of the nasal septum and medial aspects of the ethmoturbinates (same as the MMM in Figure 4 g), and (d) 23.8 ppm NA in the DMM. Arrowheads indicate the basement membrane. Negative undulation is marked by arrows. The abrupt change from necrotized to intact olfactory mucosa is marked by double arrowheads. Cilia from

olfactory receptor cells (**C**); sustentacular cells (**S**); olfactory receptor cells (**O**); basement membrane (**bm**); Bowman's glands (**bg**); arterioles (**a**); nerve bundle (**n**); dorsal medial meatus (DMM); vacuoles (******). Magnification bars = 50 μm.

4. Cellular injury from NA administered intraperitoneally. L23 is shown. NA injury occurred throughout the olfactory mucosa (g; marked in blue). Injury in the DMM at (a) 100 mg/kg and (c) 200 mg/kg NA. Injury in the MMM is shown at (b) 100 mg/kg and (d) 200 mg/kg NA. Columnar ciliated cells in the non-olfactory region (g; marked with a yellow square) after (e) 0 mg/kg and (f) 100 mg/kg NA. Arrowheads indicate the basement membrane. Dorsal medial meatus (DMM); middle medial meatus (MMM); vacuole (******). Magnification bars = 50 μm.

5. Regional differences in cytochrome P450 levels and rates of NA metabolism in microsomes isolated from rat nasal mucosa. The rate of NA metabolism is calculated from the sum of the rates of formation of both glutathione conjugates and dihydrodiol at the 160 μM of NA. (a) Lateral wall of nasal passage. The figure is adopted from Harkema et al. (1999). MT = maxilloturbinate; NT = nasoturbinate; ET = ethmoturbinates. The most dorsal ethmoturbinate was not used in order to avoid the chance of including any mucosa from the dorsal medial meatus. (b) Excised nasal septum. The septal olfactory region (SO) was distinguished from the non-olfactory region (SN) by its slightly yellowish color. The small isolated patch of olfactory mucosa situated in the septal non-olfactory mucosa (the organ of Masera) is indicated by arrow. All data are presented as the mean ± S.D., n = 3 for cytochrome P450 levels, and n = 4 for rates of NA metabolism at [S] = 160 μM.

6. NA bioactivation (**V**) versus the concentration of NA (**S**) in microsomal incubations. V is expressed in nmoles/mg of microsomal protein/min. Note the differences in scale for V.

JPET Fast Forward. Published on April 13, 2005 as DOI: 10.1124/jpet.105.084517
This article has not been copyedited and formatted. The final version may differ from this version.

FIGURE 1

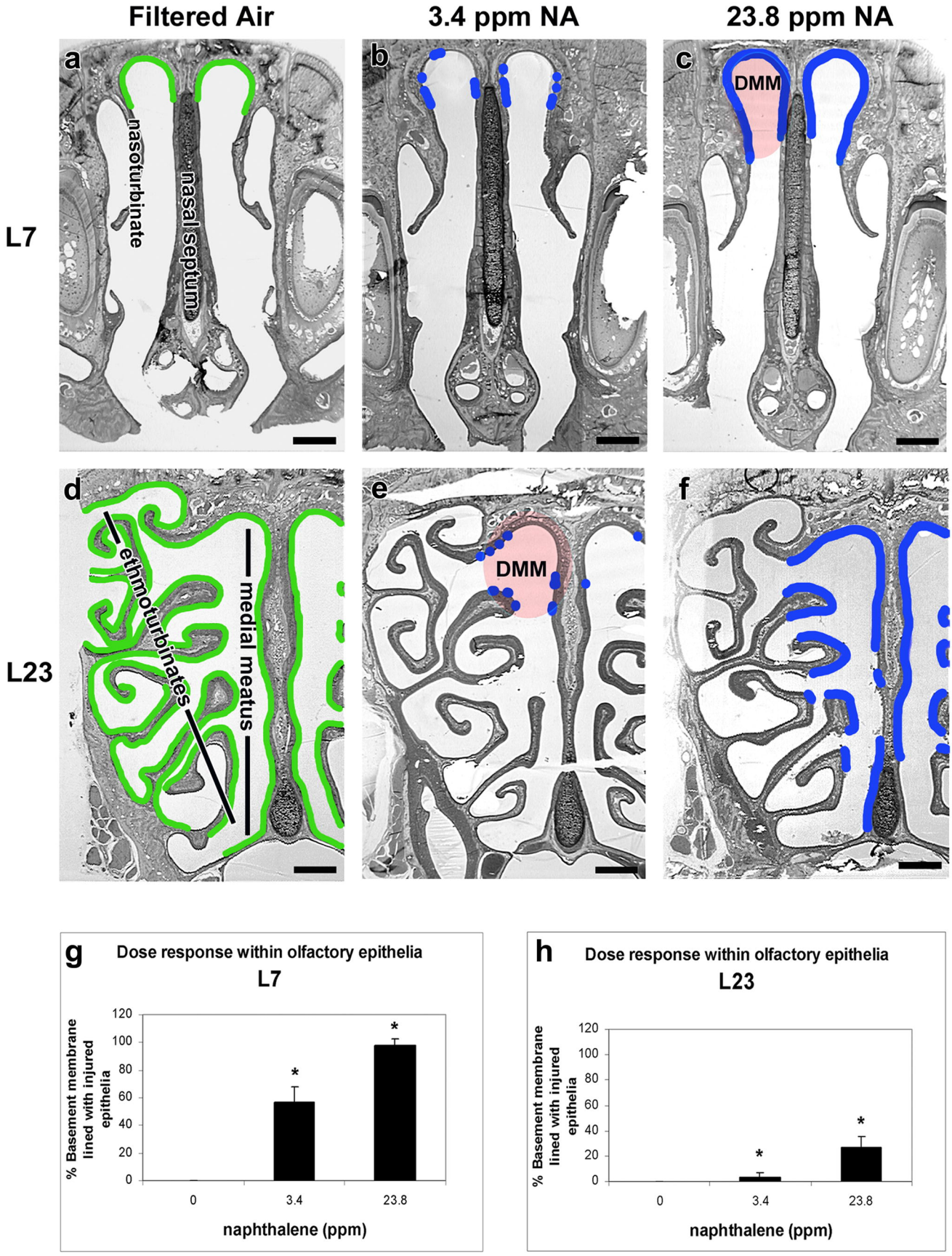

JPET Fast Forward. Published on April 15, 2005 as DOI: 10.1124/jpet.105.084517
This article has not been copyedited and formatted. The final version may differ from this version.

FIGURE 2

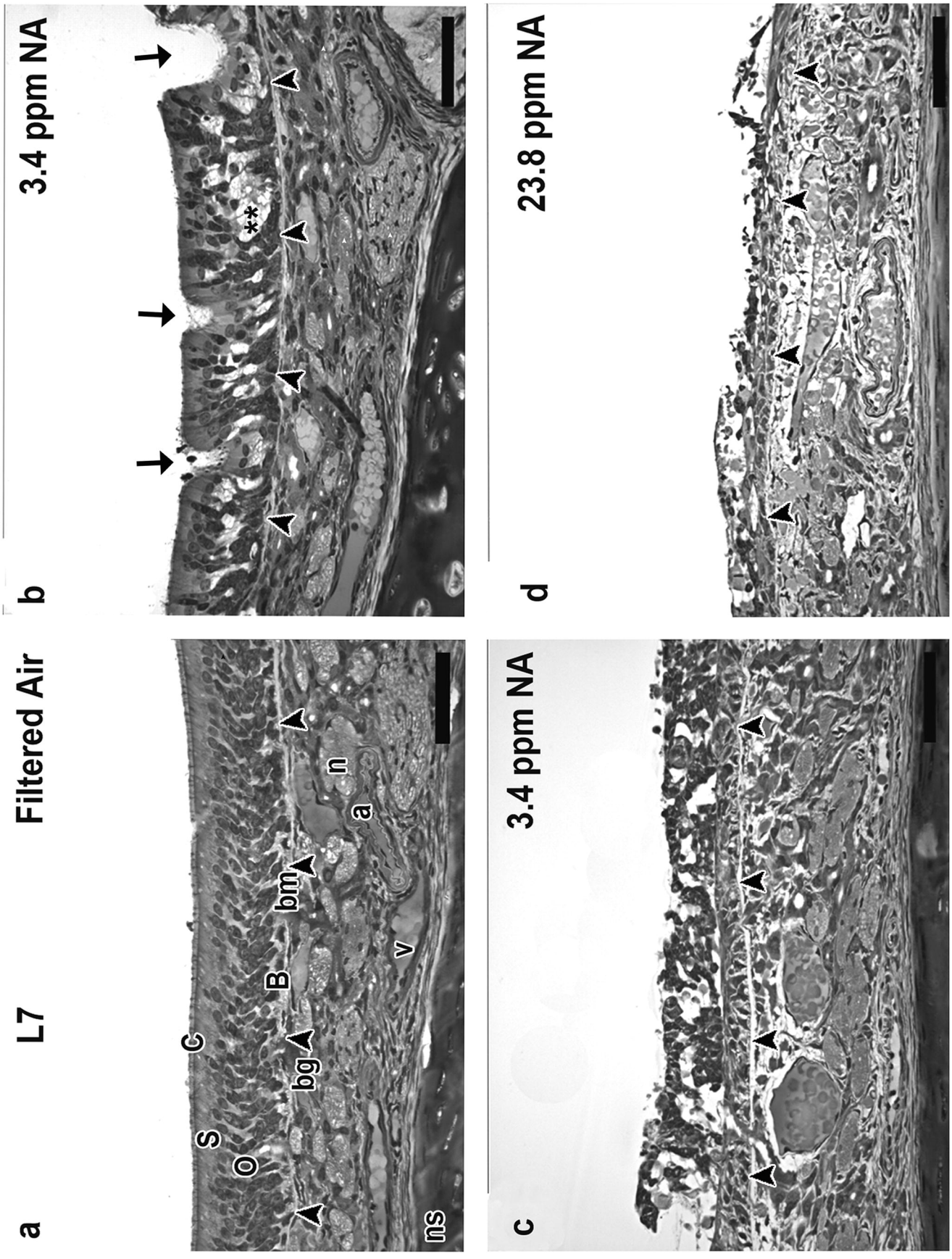

JPET Fast Forward. Published on April 15, 2005 as DOI: 10.1124/jpet.105.084517

FIGURE 3

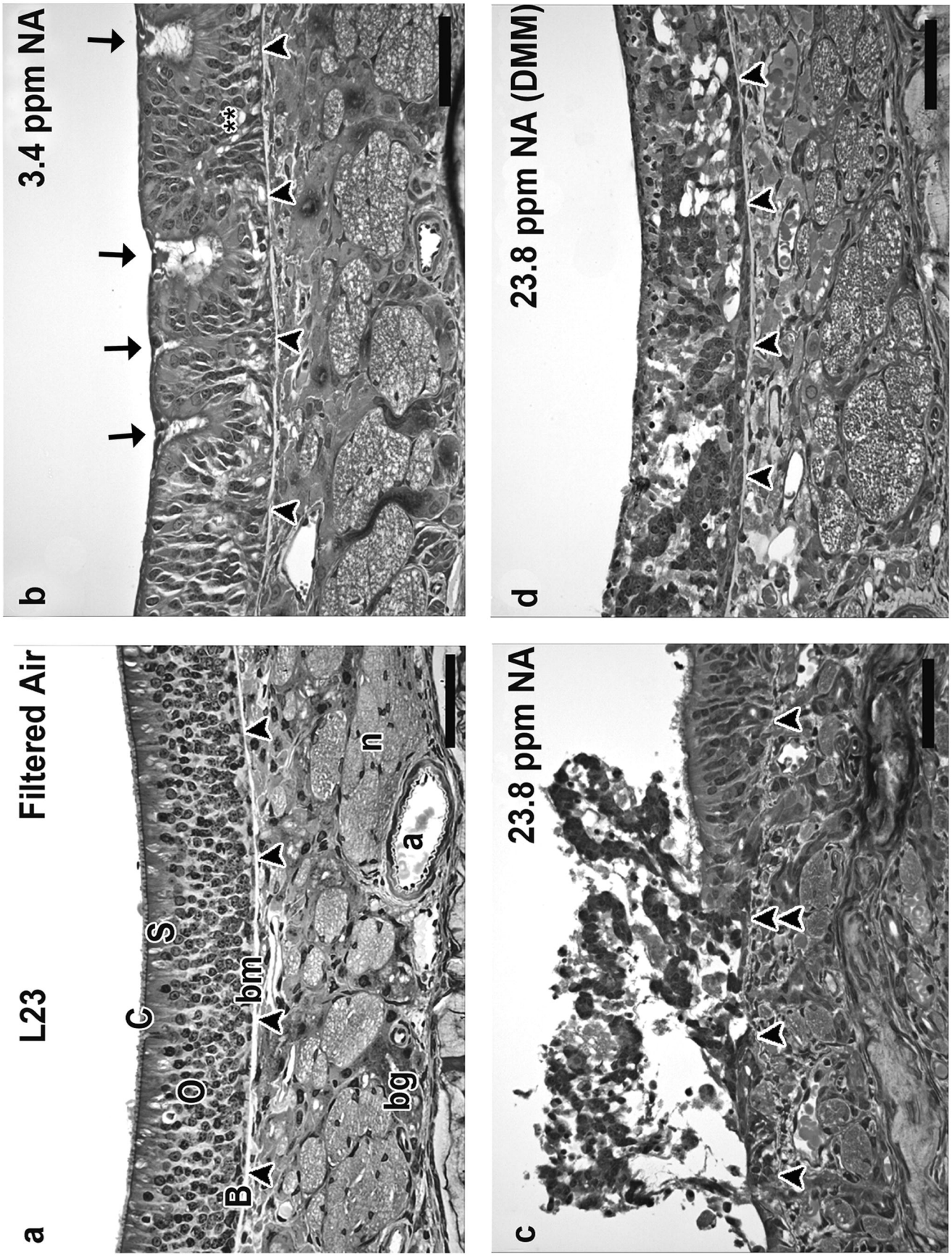

FIGURE 4

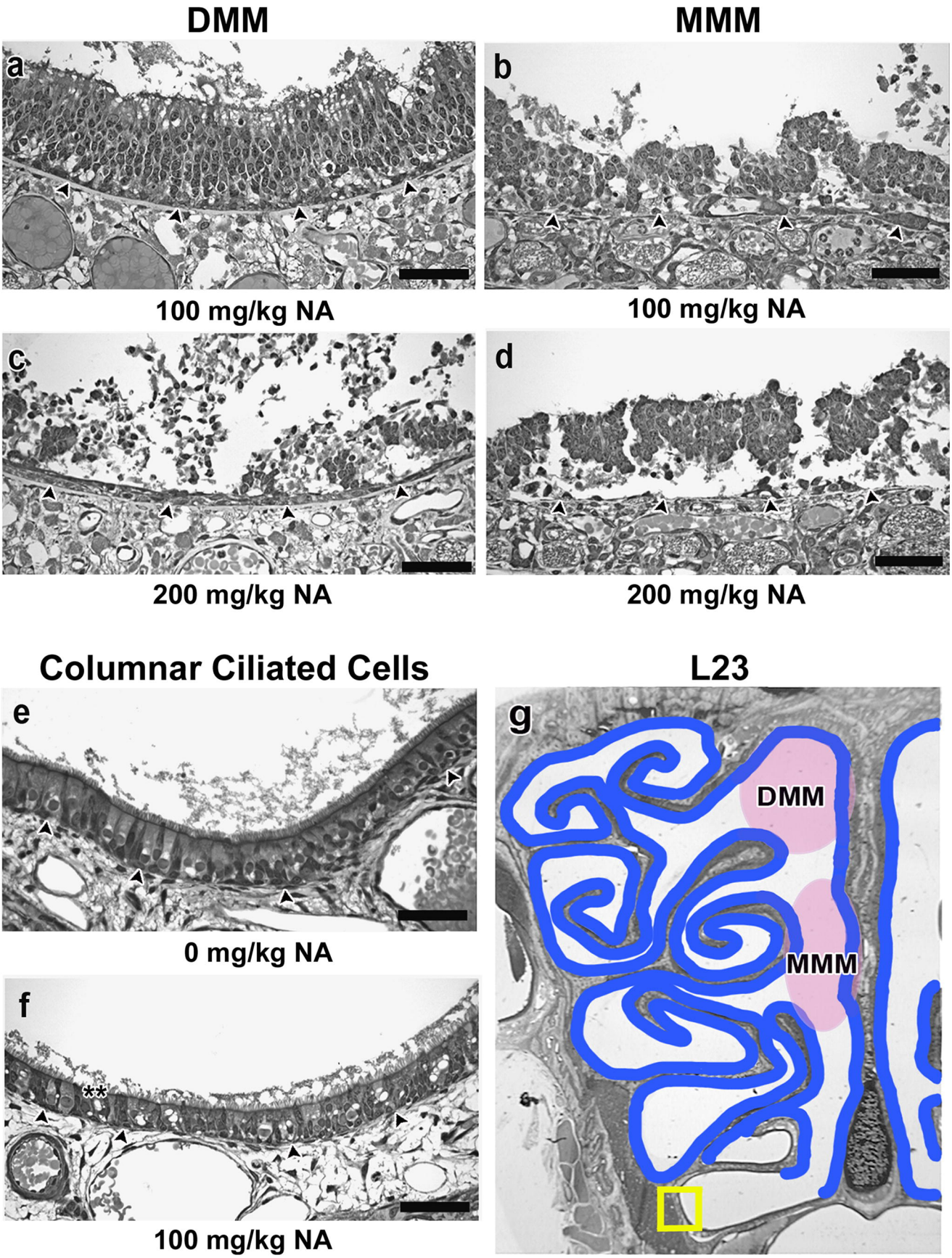

JPET Fast Forward. Published on April 15, 2005 as DOI: 10.1124/jpet.105.084517
This article has not been copyedited and formatted. The final version may differ from this version.

FIGURE 5

a

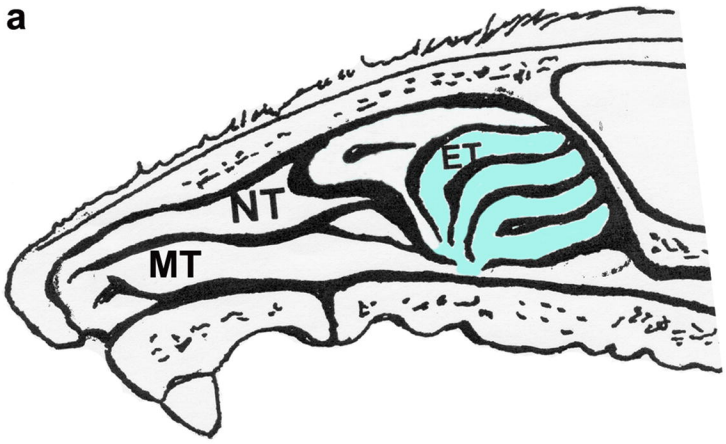

Ethmoturbinate (ET)

267 ± 11 pmoles of CYP450/mg of microsomal protein

16.8 ± 15 pmoles of NA metabolites /mg of microsomal protein/min

Septal olfactory region (SO)

278 ± 17 pmoles of CYP450/mg of microsomal protein

18.6 ± 2.4 pmoles of NA metabolites /mg of microsomal protein/min

b

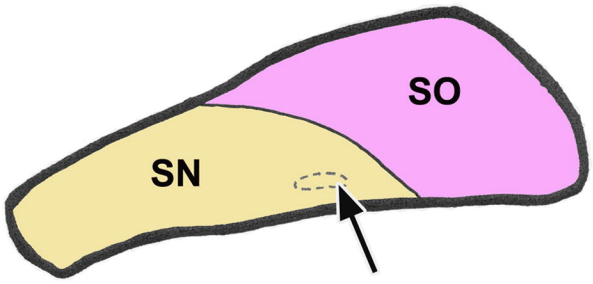

Septal non-olfactory region (SN)

74 ± 9 pmoles of CYP450/mg of microsomal protein

0.4 ± 0.1 pmoles of NA metabolites /mg of microsomal protein/min

JPET Fast Forward. Published on April 15, 2005 as DOI: 10.1124/jpet.105.084517
This article has not been copyedited and formatted. The final version may differ from this version.

FIGURE 6